"Flame Stabilization in a Concentric Conical Burner: An Integrated Experimental–Computational Study"

Mohamed k.hasanin[a], Hamdy m.Ahmed[b], Mohamed Yehia[c],Mohy S. Mansour[d]
[a,b]. higher institute of engineering, Engineering mathematics and physics department, El shorok city, Cairo, Egypt
[c,d]. Mechanical Power Engineering Department, Faculty of Engineering, Cairo University, Egypt

Abstract:-

This study investigates flame stabilization in a Concentric Flow Conical Burner (CFCB) through an integrated experimental–computational framework. The objective was to manipulate the mixing field structure to secure robust combustion stability under systematically varied operating conditions, including Reynolds number (Re), equivalence ratio (Φ), fuel composition, and mixing length. Particle Image Velocimetry (PIV) provided high-resolution velocity field measurements, while simulations employing the species transport model validated the experimental observations. A representative case at Φ = 3 and Re = 8214, with methane–air and hydrogen–air mixtures, revealed that the optimal stability occurred at LD = 10, where symmetry was sustained across an extended axial domain. The findings confirm the capacity of the CFCB to capture and reproduce fundamental stabilization mechanisms with high fidelity. Importantly, the work underscores the potential of Artificial Intelligence (AI) as a complementary tool for predictive modeling, rapid parameter optimization, and adaptive control, thereby paving the way for intelligent, data-driven burner design.

Keywords: - CFCB; Flame stability; Mixing field; AI in combustion

1-Introduction:-

Combustion is a fundamental energy conversion process in which fuels react with oxidizers to release heat and power. The efficiency and stability of this process are strongly determined by the degree of mixing between fuel and oxidizer, typically classified into three regimes: fully premixed, non-premixed (diffusion), and partially premixed combustion. Fully premixed flames provide high efficiency but suffer from flashback risks, while diffusion flames dominate industrial burners yet often exhibit high emissions. Partially premixed combustion has been repeatedly demonstrated as the most stable configuration, balancing efficiency and controllability [1,2].

Achieving robust stabilization is essential for industrial burners, and various mechanisms such as piloted flames, swirl stabilization, and reverse-flow burners have been explored [3,4]. A particularly promising design is the concentric flow conical burner (CFCB), capable of achieving combustion powers up to 250 kW in compact form [5]. The CFCB employs two co-axial tubes with a conical nozzle at the exit, creating recirculation zones that stabilize the flame. Experimental optimization has shown that cone angle, mixing length, Reynolds number (Re), and equivalence ratio (Φ) all play critical roles in determining flame stability [6]. Diagnostic tools such as planar laser-induced fluorescence (PLIF), particle image velocimetry (PIV), Rayleigh scattering, and laser-induced breakdown spectroscopy (LIBS) have been successfully applied to characterize flow, temperature, and species fields in these systems [7–9]. Most studies have focused on

methane–air mixtures, though recent work has extended to LPG, propane, and hydrogen, highlighting the relative insensitivity of conical flames to fuel type and jet velocity [10–12]. Stabilization mechanisms have been linked to recirculation zones inside the cone, which sustain flame symmetry even under turbulent conditions [13]. Yet local extinction and blowout remain challenges, particularly at high air premixing levels [14]. Computational fluid dynamics (CFD) has complemented experimental efforts, with simulations showing strong dependence of temperature, flame location, and pollutant formation on geometry, fuel type, and operating parameters [15–19]. These findings underline the versatility of the CFCB design but also point to the need for more systematic mapping of its stability mechanisms under varying turbulence and mixing conditions. Despite these advances, experimental and CFD studies face limitations in cost, resolution, and computational demand. Here, artificial intelligence (AI) offers a promising new direction. Recent work has shown that machine learning models can reconstruct flame structures from sparse data, predict pollutant emissions, and accelerate CFD calculations [20–22]. Hybrid AI–CFD frameworks have demonstrated improved predictive accuracy and reduced computational time, suggesting that AI integration could complement traditional diagnostics in analyzing complex turbulent flames [23, 24].

Motivated by these gaps, the present study applies combined experimental and computational approaches to investigate stabilization mechanisms in CFCB systems. Key parameters, including Reynolds number, equivalence ratio, mixing length, and fuel type, are systematically varied, with methane–air and hydrogen–air mixtures serving as representative cases. Particular focus is placed on a case with $\Phi = 3$ and $Re = 8214$, where results show that the most stable configuration occurs at LD = 5, sustaining symmetry over a wider axial range than other conditions. Comparisons between PIV measurements and species transport CFD models confirm the predictive accuracy of the computational approach. By linking these findings with the emerging potential of AI tools, this work highlights opportunities for integrating data-driven models with experimental diagnostics to accelerate the design of compact, high-stability burners for industrial applications.

Motivations and novelty:-This study depend on partially premixed flame condition so species transport model is preferred than diffusion or premixed model as this model apply energy and species transform equation together. Also there is research gap in applying this CFD model in this type of burner and its flame and this enhance why this model is applied. This model is important for applications which have partial premixed mixing field combustion like jet engines, steel melting furnaces, etc. Novelty of this work can appear in two items first previous researches approved that LD =5 is the most stable case for mixing field. But adding cone to burner approved that LD=10 is most favorable condition for higher stability and this result predicted by species transport model. Secondly applying PIV measurements to validate our model and results are coincided. Also there table of comparison with previous research. Another important point is that applying new fuel like hydrogen and this represent new application for this burner.

Table 1. Comparison of related literature and present study

Ref.	Burner / Method	Fuel Type(s)	Parameters Studied	Key Findings	Limitations	Present Work Contribution
[3,4]	Piloted / Reverse flow burners	Methane	Flame stabilization	Stable but limited flexibility	Geometry fixed, limited scalability	Flexible CFCB geometry allows systematic mixing control
[5,6]	Early CFCB prototypes	Methane	Cone angle, mixing length	Compact design, stability ↑ with smaller cone angle	Focused on single fuel, limited diagnostics	Broader parametric study with Re, Φ, LD, multiple fuels
[7–9]	Laser diagnostics (PLIF, LIBS, Rayleigh)	Methane	Equivalence ratio, flame structure	Enabled detailed measurements	Mostly methane only; no AI integration	Combines PIV + CFD + data-driven validation
[10–12]	Conical burners (LPG, propane, hydrogen)	LPG, propane, H_2	Fuel sensitivity, jet velocity	Conical flames less sensitive than jet flames	Not coupled with CFD validation	Comparative study of methane–air vs hydrogen–air under controlled CFCB
[15–19]	CFD (k-ε, non-premixed, reduced models)	Methane, propane, hydrogen	Re, Φ, flame temperature, CO_2	CFD useful for optimization	Expensive computation; local extinction poorly captured	Experimental validation + CFD (species transport) cross-checked
[20–24]	AI/ML in combustion	Various	Emission prediction, CFD acceleration	AI can reconstruct fields & speed up simulations	Mostly proof-of-concept; not applied to CFCB	Proposed integration of AI with CFCB diagnostics for adaptive burner design
Present Work	CFCB with PIV + CFD	Methane, H_2	Re, Φ, LD, flame stabilization	LD = 5 gives maximum stability; strong symmetry confirmed	—	First systematic CFCB study combining experiment, CFD validation, and AI integration preps

2-Experimental setup:-

The burner employed in this study is constructed from two coaxial stainless-steel tubes designed to facilitate precise control of mixing and flow conditions. The inner tube has an internal diameter of 4 mm with a wall thickness of 1 mm, while the outer tube possesses an internal diameter of 9.7 mm with the same thickness. A key feature of this design is the ability to vertically adjust the inner tube, thereby regulating the mixing length (L). This mobility also provides flexibility in interchanging the positions of fuel and air inlets, enabling systematic examination of different mixing strategies. Previous experimental investigations [11] focused on the near-tip flow field structure in the absence of a conical extension. In such cases, the analysis was limited to a region located only 2 mm above the burner exit. However, for more comprehensive assessment of the flow field using advanced optical diagnostics such as Particle Image Velocimetry (PIV), it is advantageous to incorporate a quartz conical section at the burner outlet. This modification enhances flame stability and allows for more accurate characterization of velocity and mixing distributions. The geometry of the cone was carefully optimized, with the half-cone angle fixed at 26°. Furthermore, the optimal mixing length (L) was determined to be 5 mm, while the overall burner height (H) was set to 70 mm. The nozzle exit diameter was configured at 7.3 mm to achieve a balance between flow velocity and stability [7]. In the present investigation, the mixing length is expressed as the dimensionless parameter LD, and the burner height is represented as XD. A two-

dimensional framework of analysis is adopted, emphasizing variations in both the radial (r) and axial (x) directions, in order to capture the essential features of the flow and flame dynamics.

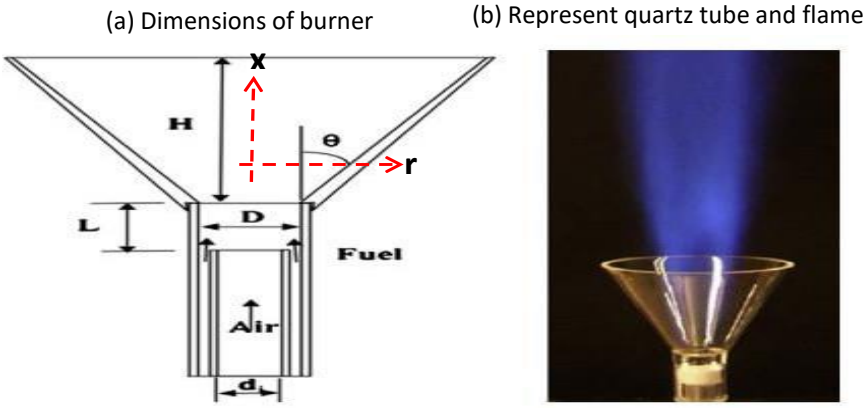

Fig (1):- represent schematic diagram for burner dimension and also with quartz nozzle

3-Methodology:-

The computational investigation presented in this work was performed using ANSYS 19, which applies the finite volume method to discretize the governing equations of the flow field. The definitions and parameters associated with the numerical approach are provided in Table (2), while the geometric specifications of the burner have been outlined in the preceding section.

Table (2):- illustrate solver model parameters

solver	2D axis symmetrical space, steady, absolute ,pressure based
Energy model	ON
Viscous model	Standard (k-ϵ), 2-equation with standard wall function
Species model	Species transport with volumetric reaction-ON

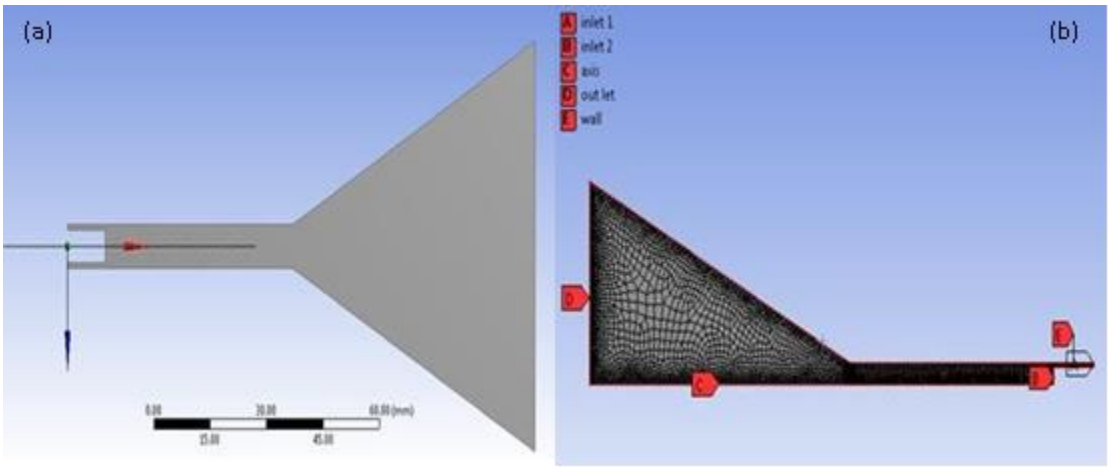

Fig (2):- (a)-geometry of burner with conical section, (b) mesh and inputs ofstudy

3.1. Geometrical Configuration

The computational model employed in this study is based on the burner configuration illustrated in Figure 2(a). The burner consists of two co-axial tubes: the inner tube serves as the inlet for fuel, while the outer tube supplies the oxidizer (air). Each inlet operates under different flow conditions, allowing variation in Reynolds numbers and equivalence ratios (Φ). The interaction between the fuel and air streams initiates in the annular region of the outer tube, where the primary mixing process begins. The mixing continues along a defined mixing length (LD) before reaching the nozzle exit, where combustion is initiated. Hence, evaluating the influence of mixing length and analyzing the characteristics of the mixture at different nozzle exit distances (XD) constitute the primary objectives of this investigation.

3.2. Computational Domain and Division

To ensure numerical stability and accuracy, the burner was divided into three distinct zones prior to meshing, as shown in Figure 3. This segmentation enabled the generation of higher-quality meshes by controlling element distribution across critical regions, including the fuel inlet, the mixing zone, and the nozzle exit. Such an approach reduces numerical diffusion and improves the representation of velocity and scalar gradients within the computational domain.

3.3. Mesh Generation

The computational grid was generated using triangular surface elements with inflation layers applied near walls to accurately capture boundary-layer behavior. Smooth transition functions were applied between coarse and fine regions to enhance element quality and minimize skew ness. The initial mesh consisted of approximately 55,000 elements and 70,000 nodes. Although this mesh provided a preliminary representation of the flow field, mesh sensitivity analysis revealed noticeable dependence of the solution on grid resolution. To mitigate this issue, progressive mesh refinement was conducted, particularly in regions with high velocity and concentration gradients. Following several iterations, an optimized mesh consisting of 168,600 elements and 170,000 nodes was adopted. This configuration achieved a balance between computational cost and solution accuracy, ensuring mesh-independent results while maintaining numerical efficiency.

3.4. Grid Independence and Validation

Grid independence tests were performed by comparing key flow parameters—such as velocity profiles, pressure drop, and scalar distributions—across successive mesh refinements. The variation between the final mesh and its coarser predecessor was found to be within acceptable limits, confirming that the adopted mesh resolution was sufficient for reliable CFD predictions. This grid independence ensured that the numerical results were not significantly influenced by discretization size, thereby enhancing the robustness of the computational methodology.

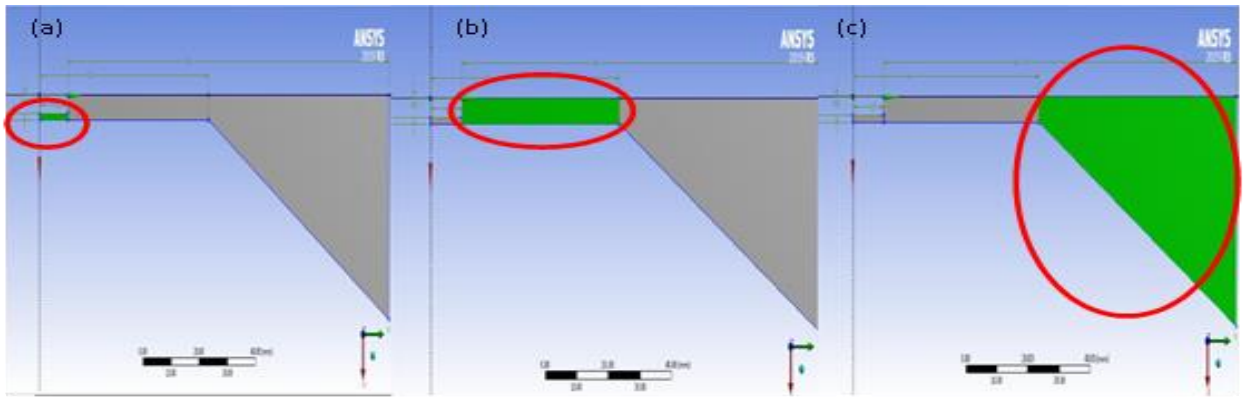

Fig. 3. Burner subdomains: (a) fuel inlet, (b) air inlet and mixing length LD, (c) conical nozzle section with nozzle-exit distance XD.

3.5:- Model and solving equations:-

The numerical simulations were performed using a pressure-based turbulent flow solver in ANSYS Fluent. Turbulence was modeled with the standard *k–ε* formulation, the governing equations of which are presented in Equations (1) and (2), as reported in [22]. This model was selected due to its robustness in predicting high Reynolds number flows with significant recirculation zones, which are characteristic of the present burner configuration.

$$\frac{\partial}{\partial t}(\rho k) + \frac{\partial}{\partial x_i}(\rho k u_i) = \frac{\partial}{\partial x_j}\left[\left(\mu + \frac{\mu}{\sigma_k}\right)\frac{\partial k}{\partial x_j}\right] + G_k + G_b + \rho\mathcal{E} - Y_M + Y_k \quad (1)$$

$$\frac{\partial}{\partial t}(\rho\mathcal{E}) + \frac{\partial}{\partial x_j}(\rho\mathcal{E} u_i) = \frac{\partial}{\partial x_i}\left[\left(\mu + \frac{\mu_t}{\sigma_\varepsilon}\right)\frac{\partial k}{\partial x_j}\right] + C_{1\varepsilon}\frac{\mathcal{E}}{k}(G_k + C_{2\varepsilon}G_b) - C_{2\varepsilon}\rho\frac{\mathcal{E}^2}{k} + S\mathcal{E} \quad (2)$$

In addition, species transport equations were incorporated to capture the detailed transport and mixing of chemical species. When coupled with the *k–ε* turbulence model, this approach provides a comprehensive representation of the combustion process. The governing equation for species transport is shown in Equation (3).

$$\frac{\partial}{\partial t}(\rho Y_i) + \nabla.(\rho\vec{v}Y_i) = -\nabla.\vec{J_i} + R_i + S_i \quad (3)$$

To accurately predict the interaction between turbulence and chemical reaction rates, the Eddy Dissipation Model (EDM) was employed. This approach requires two governing equations, as defined in [23, 24], and is widely recognized as suitable for evaluating the reaction source term, R_i Mass diffusion was modeled using Fick's law, as represented by Equation (6). However, because the present study involves turbulent flows, an extended formulation (Equation (7), as reported in [23, 24]) was applied to account for turbulent diffusion effects. The constants required for the turbulence and combustion sub-models were selected in accordance with established literature [25] and are summarized in Table 3.

$$R_{i,r} = V'_{i,r}\, M_{w,i}\, A\, \rho\, \frac{\varepsilon}{k} \min_{R}\left(\frac{Y_R}{V'_{R,r}\, M_{w,R}}\right) \quad (4)$$

$$R_{i,r} = V'_{i,r}\, M_{w,i}\, AB\, \rho\, \frac{\varepsilon}{k} \frac{\sum_p Y_P}{\sum_J^N V''_{J,r}\, M_{w,J}} \quad (5)$$

$$\vec{J_i} = -\left(\rho D_{i,m} \nabla Y_i + D_{T,i} \frac{\nabla T}{T}\right) \quad (6)$$

$$\vec{J_i} = -\left(\rho D_{i,m} + \frac{\mu_t}{Sc_t}\right) \nabla Y_i - D_{T,i} \frac{\nabla T}{T}) \quad (7)$$

3.5.1 Numerical Schemes and Solution Setup

The pressure–velocity coupling was handled using the Coupled Scheme, which provides enhanced stability and faster convergence for reacting flows. Spatial discretization of all governing equations was performed using the Second-Order Upwind Scheme to minimize numerical diffusion and ensure accuracy in regions with steep gradients. Initialization was carried out using Hybrid Initialization to establish a physically consistent starting field. The complete solution setup is presented in Table 4.

3.5.2 Boundary Conditions

The computational domain was defined with boundary conditions consistent with experimental operating conditions. The inner and outer inlets, shown in Figure 3(a) and (b), were specified as velocity inlets to prescribe mass flow rates of fuel and air, respectively. The axis of the burner was defined as a symmetry boundary. At the outlet, a pressure outlet condition was applied with a backflow turbulence intensity of 5% and a backflow viscosity ratio of 10%. The burner walls were modeled as stationary adiabatic walls with standard roughness specifications. These boundary conditions are summarized in Table 5.

Table (3):- Model constants used in the simulations

(k-ϵ) model parameters	Magnitude
C_μ	0.09
$C_{1\varepsilon}$	1.44
$C_{2\varepsilon}$	1.92
PrTKE	1
PrTDR	1.3
PrEnergy	0.85
PrWall	0.85

Sc_t	0.7
Eddy dissipation parameters	
A	0.4
B	0.5

Table (4):- illustrate solving system and boundary conditions

Parameters	Solving scheme
Scheme used	couple
Spatial Discretization	
Pressure	Second-Order Upwind
Momentum	Second-Order Upwind
Turbulent Kinetic Energy	Second-Order Upwind
Turbulent Dissipation Rate	Second-Order Upwind
CH4/O2/CO2/H2O/Energy	Second-Order Upwind
Solution Initialization	Hybrid Initialization

Table (5):- boundary conditions of burner

Parameters	Conditions
A-inlet (1)	Velocity inlet
B- inlet(2)	Velocity inlet
C- axis	Axis symmetry
D-out-let	Pressure out let with ,Backflow Turbulent Intensity: 5% Backflow Turbulent Viscosity Ratio: 10%
E- wall	Stationary Wall with Standard Wall Roughness

4. Results and Conclusions

4.1 Stability Mapping

The stability of the burner was first investigated to identify operating conditions suitable for reliable combustion. The principal control parameter in this analysis was the mixing length (LD), which defines the region where fuel and air streams interact prior to entering the nozzle. In addition, the inner fuel velocity and the outer air velocity were independently varied, and their influence was characterized through Reynolds numbers. Although both the inner Reynolds number (Re_{in}) and outer Reynolds number (Re_{out}) could be considered, a more comprehensive description of the jet was achieved by defining a mixture Reynolds number, calculated on the basis of jet velocity. The fuel-to-air ratio was expressed through the jet equivalence ratio (Φ).

The stability map of the burner, presented in Figure 4, highlights the conditions under which stable and unstable flames were observed. From this map, a stable operating point was selected at Φ=3, Re=8214, and LD=5. This condition was adopted as the reference case for subsequent CFD

simulations, ensuring that the numerical analysis was conducted under experimentally confirmed stable conditions.

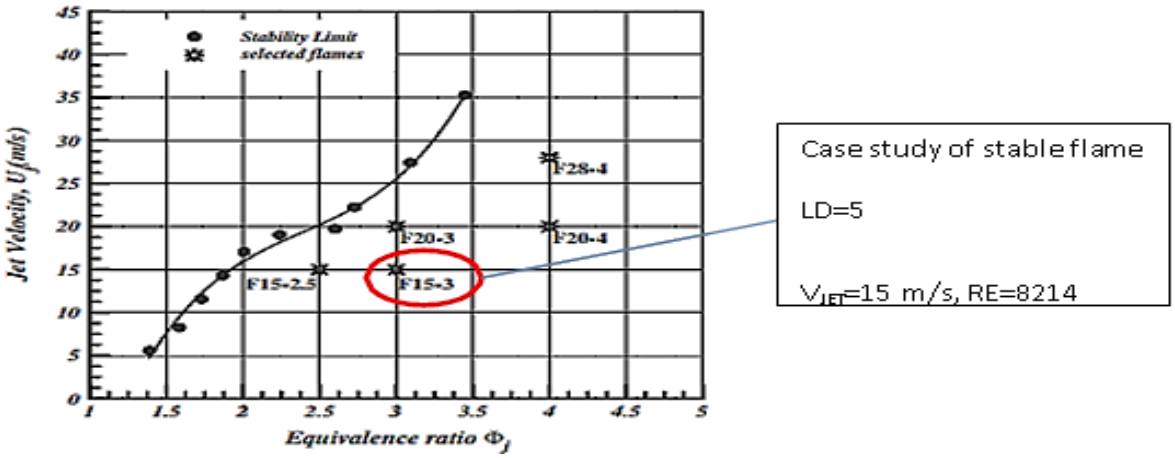

Fig. 4. Stability curve of the CFCB at LD=5. The red circle indicates the selected operating condition adopted for the case study.

4.1.1 Model Validation with PIV

Validation of the CFD model against experimental data was essential to establish confidence in the simulation results. Particle Image Velocimetry (PIV) was employed to measure velocity fields within the burner. The results revealed the existence of a backflow region of air in proximity to the conical wall, where eddies were formed. These recirculation zones acted as a self-stabilization mechanism for the flame, promoting anchoring and sustained combustion.

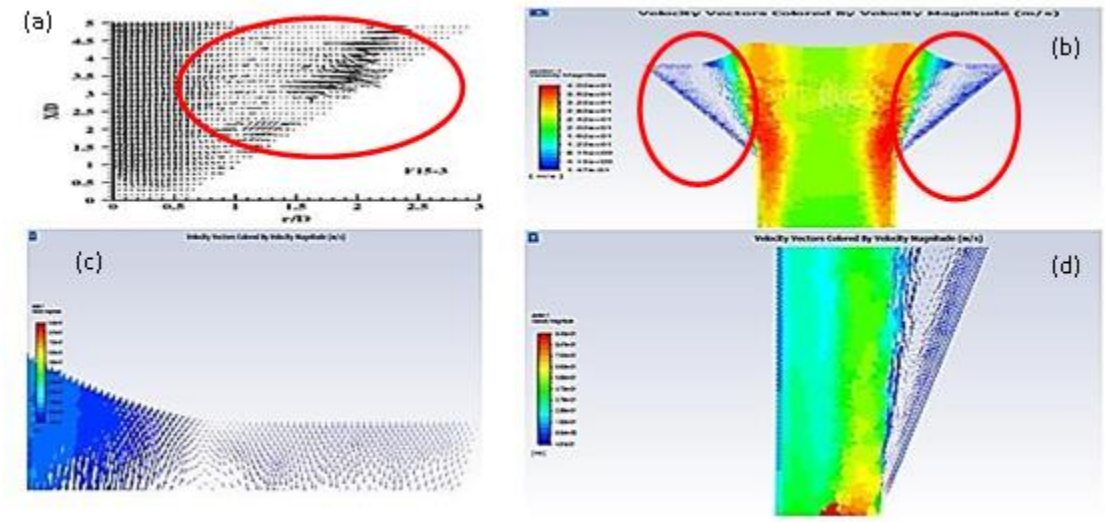

Fig. 5. Flow-field validation: (a) PIV measurements showing recirculation eddies responsible for burner stabilization; (b) CFD prediction of the same region; (c–d) magnified views highlighting the stabilization zone.

Figure 5 illustrates a comparison between the PIV measurements and CFD predictions. The close agreement between the two datasets confirmed that the numerical model was able to reproduce the principal flow structures observed experimentally. In particular, the prediction of the recirculation region validated the turbulence–combustion interaction captured by the chosen models. This step was crucial in demonstrating the reliability of the computational framework prior to conducting further parametric studies.

4.2 different effects of parameters

Following validation, a series of numerical simulations were carried out to investigate the influence of key operating parameters. Different mixing lengths (LD) were examined at fixed nozzle exit locations (XD) to evaluate the role of fuel–air interaction length on flame stabilization and combustion characteristics.

Additionally, the effects of equivalence ratio (Φ) and Reynolds number were systematically analyzed for different fuel compositions. These parametric studies provided insight into the interplay between jet momentum, mixing intensity, and combustion stability. The solver configuration and boundary conditions employed in this stage of the analysis are summarized in Tables 3 and 4.

4.2.1 Flow field velocity effect of LD:-

At the operating condition of Re=8314, Φ=3, and axial distance XD=0, the effect of varying the mixing length LD on the velocity field and temperature distribution was systematically investigated, as illustrated in Fig. 6. The results reveal a clear dependence of near-wall flow structures on LD. At the lowest mixing length, the velocity and temperature profiles exhibit relatively flat distributions adjacent to the wall. With increasing LD these distributions evolve into sharp peaks, indicating intensified gradients and enhanced mixing in the boundary region. As LD continues to increase, the profiles gradually return to a flatter form, suggesting the onset of flow re-stabilization and homogenization.

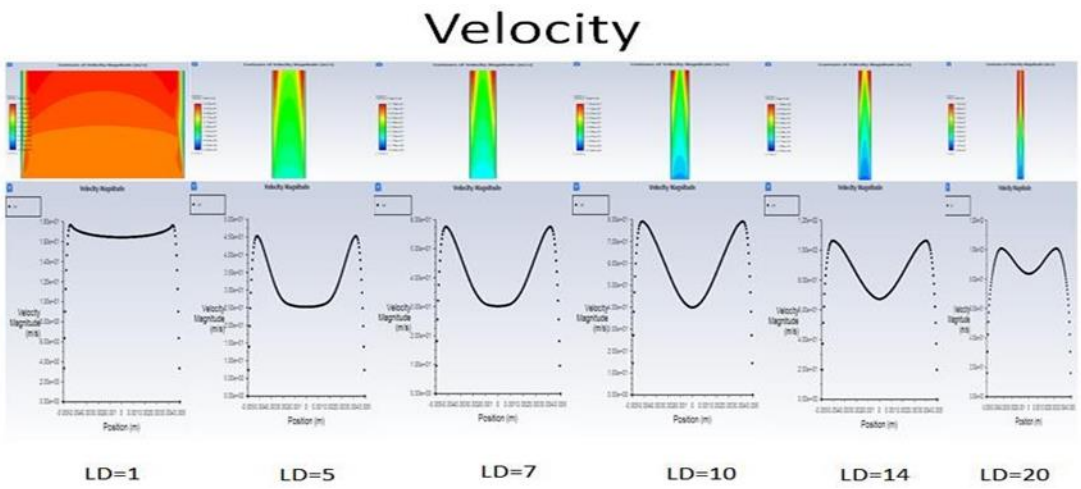

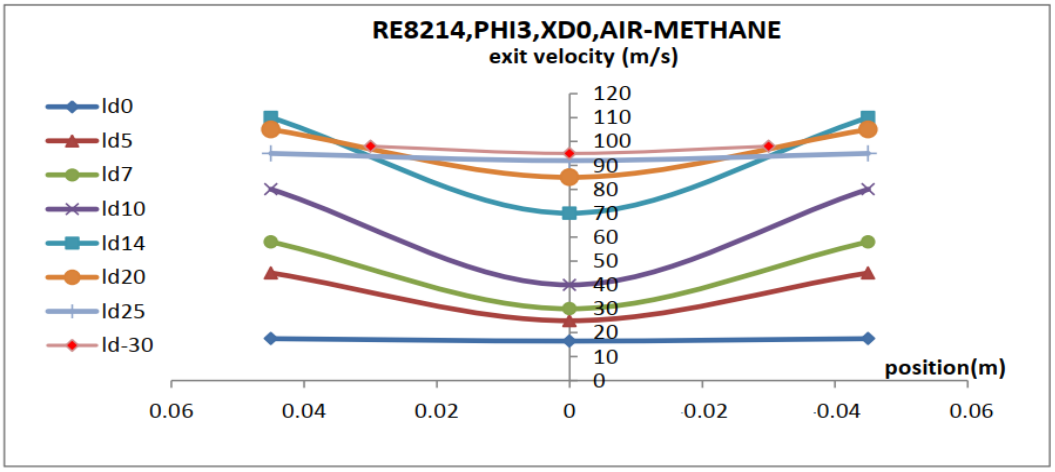

Fig. 6. Exit velocity distribution profiles of the burner at varying mixing lengths (LD).

This graph illustrates how exit velocity distribution varies across different operating conditions in an air-methane flow system. The diversity in velocity profiles reflects changes in flow dynamics—ranging from uniform jets (Id0, Id-30) to highly non-uniform, swirling flows (Id14, Id20). The central dip in velocity for most cases suggests the presence of a low-velocity core, potentially indicative of recirculation zones important in combustion stability and mixing efficiency. Such data is critical for optimizing combustor design, ensuring proper fuel-air mixing, minimizing NOx emissions, and improving flame stability. The choice of configuration (e.g., Id14 vs. Id0) would significantly impact performance based on desired velocity profiles and mixing characteristics.

4.2.2:- Flow field velocity effect of XD:-

The influence of increasing axial distance XD was examined at Re=8214and Φ=3, with a focus on the conical section and a representative mixing length of LD=5, as illustrated in Fig. 7. The results indicate that, under these conditions, the flow field progressively shifts away from the centerline, producing an asymmetric velocity distribution. This asymmetry can be attributed to pressure imbalance, with reduced pressure on the displaced side and elevated pressure on the opposite side. Furthermore, the deviation occurs more rapidly at LD=10, emphasizing the sensitivity of flow stability to mixing length. To address this, the optimal axial distance that preserved symmetry across different LDvalues was identified as XD=1. As demonstrated in Fig. 8, the velocity profile remains symmetric even at larger mixing lengths, extending up to LD=10.

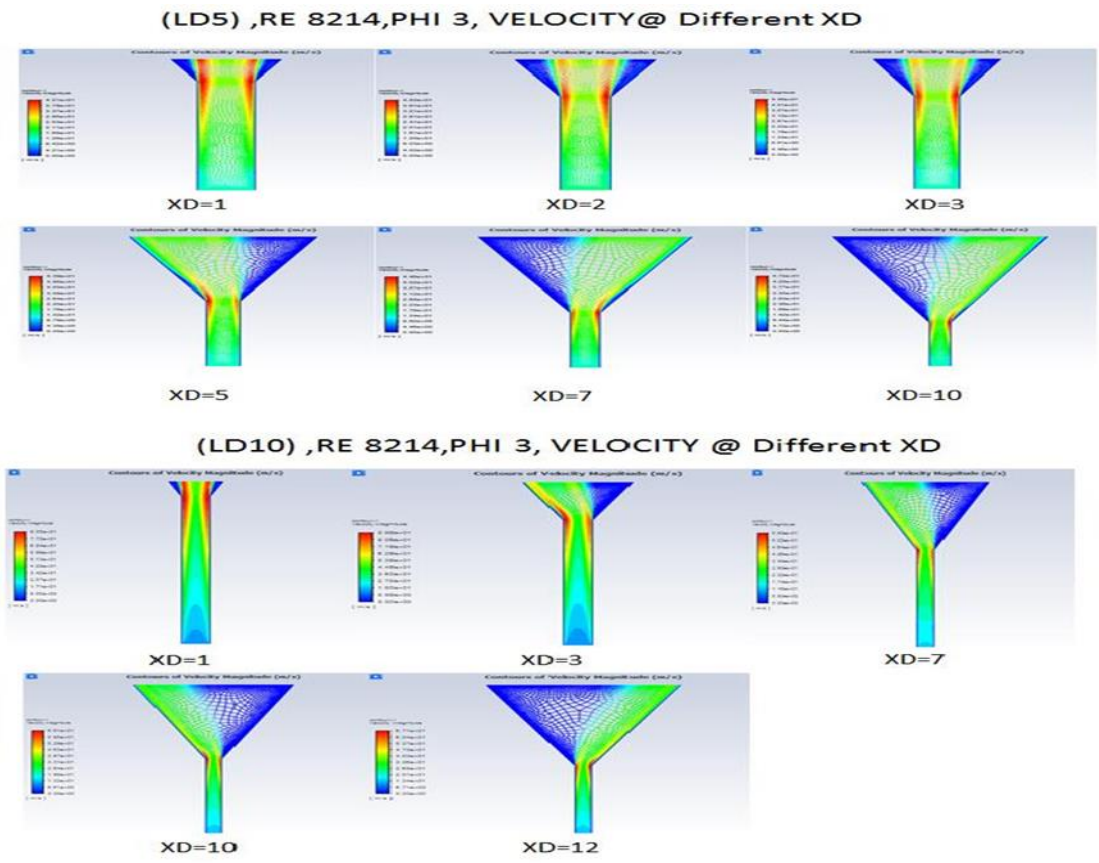

Fig (7):- comparison between different LD =5&10 for different XD

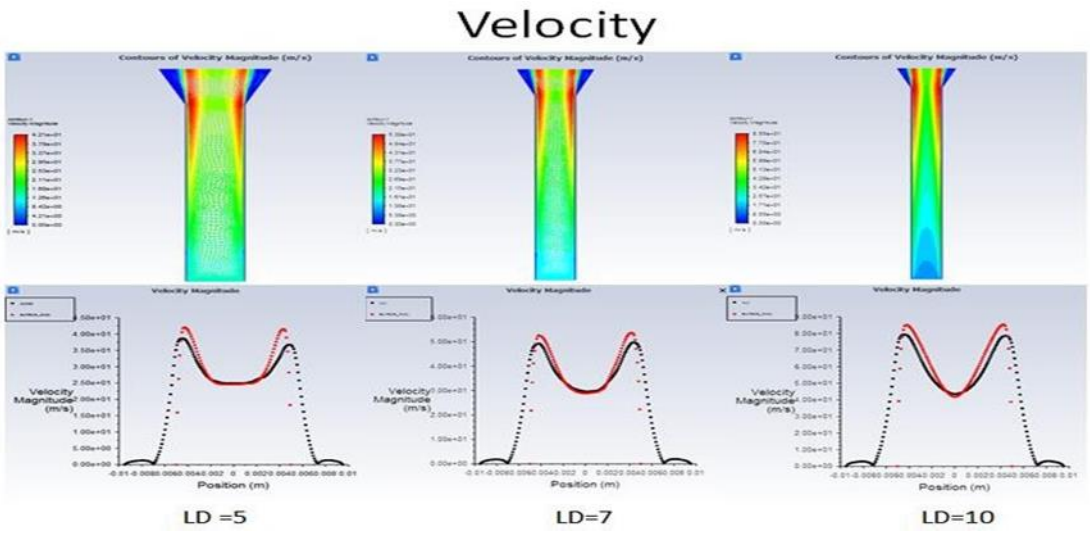

Fig (8):- illustrate symmetry of velocity profile at XD=1 for different LD

This figure (8) effectively illustrates how increasing the length-to-diameter ratio (LD) improves the velocity uniformity and flow quality in a confined flow system. As LD increases from 5 to 10: The velocity profile becomes smoother and more symmetric. Peak velocities are moderated, but flow stability and uniformity improve. The contours show better expansion and less distortion, suggesting reduced turbulence and separation. Thus, LD = 10 represents the most favorable condition for achieving well-developed, uniform flow, making it ideal for applications where consistent velocity distribution is critical—such as in premixed combustion, mixing chambers, or aerodynamic nozzles.

4.2.3:- Flow field temperature effect of LD:-

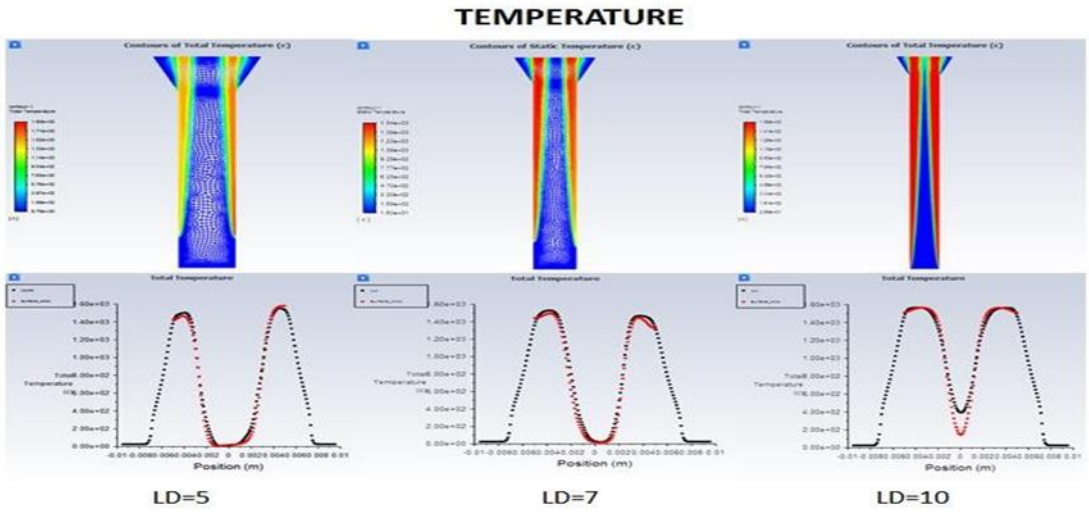

Fig. 9. Temperature distribution at XD=1 for varying mixing lengths (LD)

The figure (9) compares temperature distributions for LD = 5, 7, and 10 in a combustion system, showing that increasing the length-to-diameter ratio improves thermal uniformity. Higher LD values result in smoother, more symmetric temperature profiles with reduced gradients and localized hot spots. Contour plots reveal better heat distribution and less edge cooling at higher LD, indicating enhanced mixing and flame stability. The LD = 10 case demonstrates the most uniform temperature field, suggesting optimal combustion performance. These findings highlight that longer nozzles promote stable, efficient burning by allowing full flow development and improved heat retention, making them preferable for applications requiring low emissions and high efficiency.

4.2.4:- Effect of fuel type

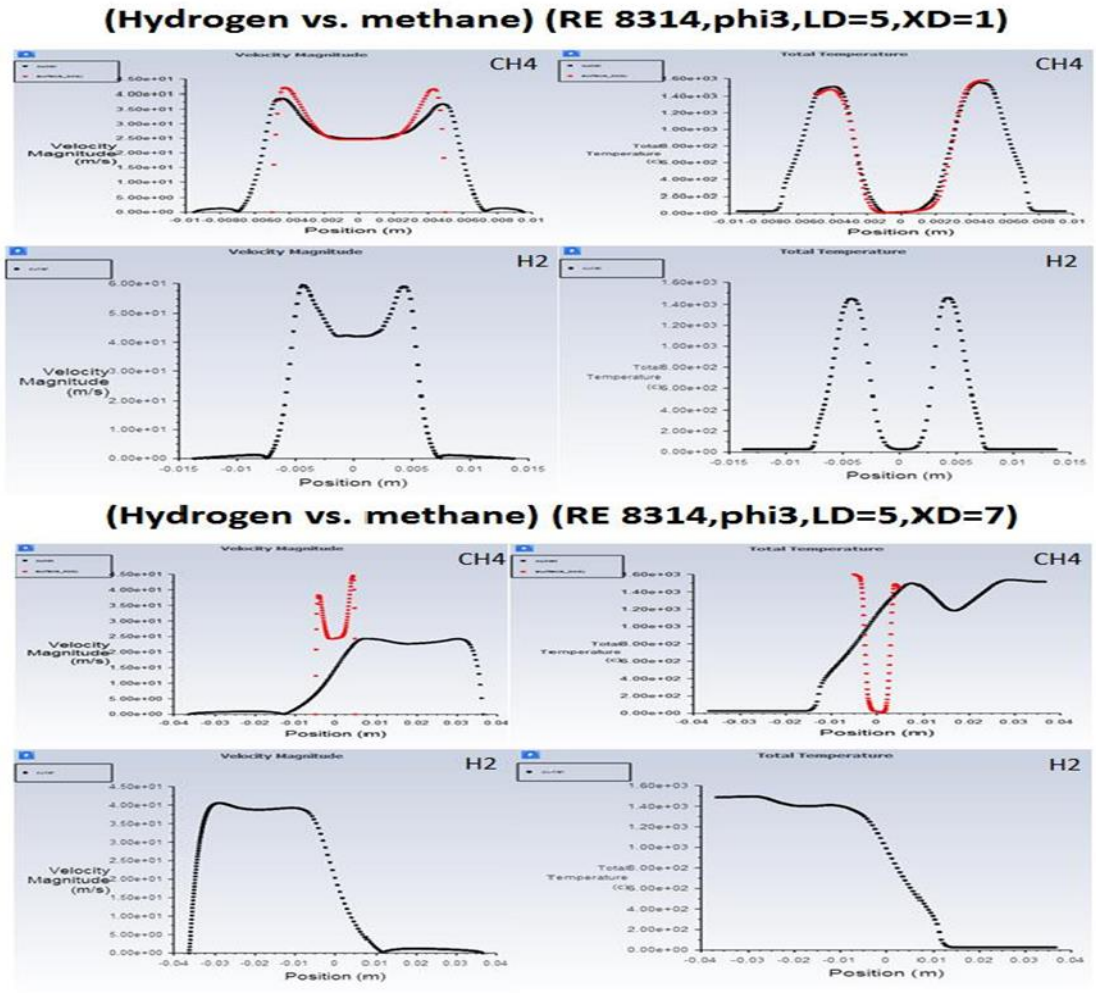

Fig. 10. Velocity and temperature profiles for methane–air and hydrogen–air combustion in a coaxial burner, illustrating the influence of mixing length LD and axial distance XD.

Figure (10) has provided a comparative analysis of methane–air and hydrogen–air combustion in a coaxial burner, with a particular focus on the effects of mixing length LD and axial distance XD on velocity and temperature distributions. Methane, the principal component of natural gas, was used as the benchmark fuel due to its established role in combustion research. At moderate LD, methane exhibited relatively stable flame structures; however, at extended mixing lengths, its velocity and temperature profiles developed central dips and asymmetries, suggesting recirculation zones and a decline in flame stability. In contrast, hydrogen demonstrated greater uniformity and resilience across a wider range of geometrical configurations. While its lower density and higher flame speed produced sharper velocity and temperature gradients at short LD, hydrogen maintained symmetric and sustained distributions at longer mixing lengths, thereby avoiding the instabilities observed with methane. These results highlight hydrogen's potential advantages in systems with extended residence times, where stability and efficiency are critical. Nonetheless, hydrogen's high reactivity also poses challenges, most notably its strong tendency toward

flashback. This phenomenon destabilizes the flame by promoting upstream propagation of the burning front, particularly in cone-stabilized burners. Consequently, while hydrogen offers clear benefits as a low-carbon alternative to methane, its practical deployment requires careful burner design and control strategies to mitigate flashback risk. Overall, the findings reinforce hydrogen's promise as a sustainable energy carrier, while emphasizing that burner geometry, operating conditions, and stabilization mechanisms must be optimized to fully exploit its combustion advantages.

5:-conclusion:-

This study examined flame stabilization in a Concentric Flow Conical Burner (CFCB) using an integrated experimental–computational approach. While experimental studies on this burner are extensive, computational investigations remain limited. The present work confirmed that the species transport model provides a reliable, low-cost diagnostic tool, reproducing velocity and temperature fields in strong agreement with Particle Image Velocimetry (PIV) measurements. The conical geometry promoted recirculation zones that enhanced flame stability by generating reverse flow similar to swirl effects. Stability was strongly influenced by operating conditions, particularly Reynolds number Re, equivalence ratio Φ, mixing length LD, and axial distance XD. The most stable case was observed at XD=1 with LD=10, where symmetrical velocity and temperature profiles were sustained. Fuel comparison showed methane to be more stable than hydrogen due to its lower reactivity, although both were well captured by the model. These findings validate the CFCB as a robust platform for combustion studies and highlight opportunities for future work, including three-dimensional analysis and AI-assisted burner optimization. Future work will be applying species transport model as three dimension coordinates also applying new mixture like hydrogen and ammonia also biogas. Make more experimental study and try to change geometry and burner design

References:-

[1] R.W. Bilger, combust. Sci .Technol 13(1976) 155-170.

[2] Peters, N. 2000. Turbulent Combustion Cambridge University Press Cambridge, UK.

[3] Mansour, M.S et al, (1989) A Reverse Flow Reactor for Turbulence/Chemistry Interaction Studies, Combustion Science and Technology, 65:1-3, 83-101

[4] Masri, A.R. 2015. Partial premixing and stratification in turbulent flames. Proc.Combust. Inst., 35, 1115–1136
.
[5] M.S.Mansour, Combust.Sci.Technol152 (2000)115–145.

[6] Masri, A.R. 2015. Partial premixing and stratification in turbulent flames. Proc.Combust. Inst., 35, 1115–1136

[7] Fawzy El-Mahallawy, Ahmed Abdelhafez Mohy S. Mansour (2007) Mixing and

Nozzle Geometry Effects on Flame Structure and Stability, Combustion Science And Technology, 179:1-2, 249-263

[8] B. Li et al. / Proceedings of the Combustion Institute 32 (2009) 1811–1818

[9] M.S. Mansour et al. / Spectrochimica Acta Part B 64 (2009) 1079–1084

[10] B. Yan et al. / Experimental Thermal and Fluid Science 34 (2010) 412–419

[11] Mansour, M.S., Elbaz, A., and Samy, M. 2012.The stabilization mechanism of highly stabilized partially premixed flames in a concentric flow conical nozzle burner. Exp. Therm. Fluid Sci., 43, pp. 55–62.

[12] E. Baudoin Flow Turbulence Combust (2013) 90:269–284

[13] A.M. Elbaz et al. The flow field structure of highly stabilized partially premixed flames in a concentric flow conical nozzle burner with co-flow, Exp. Therm. Fluid Sci. (2015)

[14] M.S. Mansour et al., Effect of the mixing fields on the stability and structure of turbulent partially premixed flames in a concentric flow conical nozzle burner,Combustion and Flame (2016)

[15] Elbaz, A.M., Experimental Thermal and Fluid Science (2018), https://doi.org/10.1016/j.expthermflusci.2018.01.010

[16] A.S. Nair, B. Mohan Krishna and S. Ajith Kumar, Study of non – Premixed combustion of propane and methane using CFD,Materials Today: Proceedings, https://doi.org/10.1016/j.matpr.2020.09.713

[17] Guessab Ahmed, Aris Abdelkader, Abdelhamid Bounif, Iskander Gökalp Reduced chemical kinetic mechanisms: Simulation of turbulen non-premixed CH4-air flame, Jordan J. Mech. Ind. Eng., Volume 8 Number 2, April. 2014 ISSN 1995-6665.

[18] Wang, Shixuan, Zili Yuan, and Aiwu Fan. "Experimental investigation on nonpremixed CH4/air combustion in a novel miniature Swiss-roll combustor." Chemical Engineering and Processing-Process Intensification 139 (2019): 44-50.

[19] Aikun Tang, Yiming Xu, Chunxian Shan, Jianfeng Pan, Yangxian Liu, A comparative study on combustion characteristics of methane, propane and hydrogen fuels in micro-combustor, School of Energy and Power Engineering, Jiangsu University, Zhenjiang 212013, China.

[20] Lucky Anetor, Edward Osakue, Christopher Odetunde, Reduced mechanism approach of modeling premixed propane-air mixture using ANSYS fluent, Eng. J. Volume 16 Issue 1

[21] Mr. Ankit Rajak, Mr. Amit Datta, Mr. Vishwajeet Kureel, Analysis of combustion characteristics of methane/air mixture in coaxial combustor, Int. J. Adv. Res. Sci. Eng.,Vol.no.5, Issue-2015

[22] A.S. Nair, B. Mohan Krishna and S. Ajith Kumar, Study of non – Premixed combustion of propane and methane using CFD,Materials Today: Proceedings, https://doi.org/10.1016/j.matpr.2020.09.713

[23] Wan, Jianlong, Yongjia Wu, and Haibo Zhao. "Excess enthalpy combustion of methane-air in a novel micro non-premixed combustor with a flame holder and preheating channels." Fuel 271 (2020): 117518.

[24] Mikulčić, Hrvoje, Jakov Baleta, Xuebin Wang, Jin Wang, Fengsheng Qi, and Fan Wang. "Numerical simulation of ammonia/methane/air combustion using reduced chemical kinetics models." International Journal of Hydrogen Energy (2021).
[25] ANSYS Modeling and Meshing Guide002114 November 2004 ANSYS, Inc. is a UL registered ISO 9001: 2000 Company